



Research paper

Influence of mechanical pre-consolidation of soil on the assessment of stress level in geotechnical practice

Mirosław Bukowski¹, Rafał Kuszyk², Maciej Maślakowski³

Abstract: Geotechnical design includes construction works in the course of which the soil is subjected to vertical repetitive stress in the process of compacting, for example in the case of embankments or landfills. When the stress exceeds the pre-consolidation threshold there emerges accumulation of permanent deformation, usually horizontal, which causes additional lateral stress. A rule verified by long-term practical use was presented for to determine the horizontal stress resulting from mechanical pre-consolidation. Independent mathematical analysis has confirmed that the boundary ranges of the cyclic lateral stress factor correspond to the active or reactive states of strain. In geotechnical practice it is the reactive states, in which additional accumulation of lateral strain occurs in soil, that are important.

Keywords: dynamic consolidation, glacier consolidation, mechanical compaction, preconsolidation

¹Ph.D., Warsaw University of Technology, Faculty of Civil Engineering, Al. Armii Ludowej 16, 00-637 Warsaw, Poland, e-mail: miroslaw.bukowski@pw.edu.pl, ORCID: 0009-0005-3037-6679

²Ph.D., Warsaw University of Technology, Faculty of Civil Engineering, Al. Armii Ludowej 16, 00-637 Warsaw, Poland, e-mail: rafal.kuszyk@pw.edu.pl, ORCID: 0000-0001-8657-1215

³Ph.D., Warsaw University of Technology, Faculty of Civil Engineering, Al. Armii Ludowej 16, 00-637 Warsaw, Poland, e-mail: maciej.maslakowski@pw.edu.pl, ORCID: 0000-0002-2946-1594

1. Introduction

Geotechnical practice includes construction works or structures in the course of which the soil is subjected to vertical repetitive stress in the process of compacting or exploitation, for example in the case of road or railway embankments, landfills etc. When the stress exceeds the pre-consolidation threshold σ_p there emerges accumulation of permanent deformation, usually horizontal, which causes additional lateral stress. The standards for retaining wall design [13] recommend that the backfill with a width of up to 1.5 m should account for increased earth pressure at rest, depending on the type of soil and the soil compacting equipment. The recommendations of the standards for flat deformation state are justified in [8]. The general issues related to determining the degree of pre-consolidation are highlighted in [12]. Mechanical pre-consolidation brings the stress level in the soil to the level of yield surface in idle state, which is well illustrated by the graph in Fig. 1, based on [18].

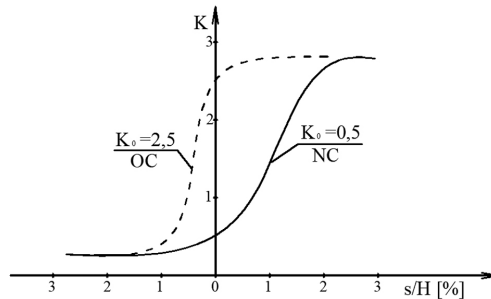


Fig. 1. Relation between the lateral stress ratio and the shift in relation to the retaining wall [18]

A rule verified by long-term practical use was searched for to determine the horizontal stress resulting from mechanical pre-consolidation. The semi-empirical Dorman-Edwards rule [9] was adopted which related to permitted stress caused by repetitive loads on the soil half-space in road construction business:

$$(1.1) \quad \sigma_{\text{dop}} = \frac{0,006E}{1 + 0,7 \lg n}$$

where E is the initial soil deformation modulus; n – the number of load cycles.

The form of this formula is derived from a generally known formula which describes the settlement of elastic half-space (the deformation method):

$$(1.2) \quad s = \frac{\sigma_{\text{dop}} B(1 - \nu^2)\omega}{E}$$

Based on the experience $\frac{s}{B(1-\nu^2)\omega} = 0,006$ was adopted, which leads to the formula (1.1), in which the module, following a load cycle, is:

$$(1.3) \quad E_n = \frac{E}{1 + 0.7 \lg n}$$

Total strain is expressed as $\varepsilon = \varepsilon_s + \varepsilon_p$, where ε_s and ε_p are respectively the elastic and the fixed /permanent parts. The sum sign means that the strain components are combined in a series, and they emerge because of uniform strain σ . Hydrostatic state of strain was assumed in the part where permanent deformation occurs, by analogy to the elastic-plastic solutions for load capacity of foundations. The lateral stress ratio defines the relation of the accumulated permanent/fixed horizontal stress $\Delta\sigma_{xi}$ to vertical stress σ_z . Using the principle of hydrostatic distribution of stress, the lateral stress ratio K_C for repetitive loads is:

$$(1.4) \quad K_C = \frac{\sum_1^n \Delta\sigma_{xi}}{\sigma_z} = \frac{\sum_1^n \Delta\varepsilon_i}{\varepsilon_1}$$

where $\Delta\varepsilon_i$ denotes the growth of fixed/permanent strain starting from load cycle i , ε_1 is the vertical strain during the first load cycle. While accounting for the Hooke’s law and the formula (1.3), the relation (1.4) can be expressed in the following form:

$$(1.5) \quad K_C = \sum_1^n \left| \frac{1}{1 + 0,7 \lg(i + 1)} - \frac{1}{1 + 0,7 \lg i} \right|$$

The norm symbol has been introduced to eliminate negative values in the series. To make the notation concise, the expressions in the norm are denoted by a_i , which leads to $K_C = \sum_1^n |a_i|$. The convergence of the series (1.5) has been estimated using Cauchy criterion (concerns the non-negative expressions a_i):

$$(1.6) \quad F \leq \sum_1^n |a_i| \leq a_1 + F$$

where F is the limit of the improper integral $F = \int_1^\infty f(x) dx = F_n$. For operating purposes, it is more convenient to express equation (1.5) as:

$$(1.7) \quad K_C = \sum_1^n \left| \frac{0,7 [\lg(i + 1) - \lg i]}{(1 + 0,7 \lg i)(1 + 0,7 \lg(i + 1))} \right|$$

Using (1.7), with partial replacement of \lg by \ln , the limits of the estimate, calculated using formula (1.6), will be:

$$(1.8) \quad \frac{0,7 \ln 2 \ln 10}{\ln 20} \approx 0,40 \leq K_C \leq 1 + \frac{0,7 \lg 2}{1 + 0,7 \cdot 0,3} \approx 1,2$$

Independent mathematical analysis has confirmed that the boundary ranges of the cyclic lateral stress factor correspond to the active or reactive states of strain. In geotechnical practice it is the reactive states, in which additional accumulation of lateral strain occurs in soil, that are important. Additional lateral strain, $\sum \Delta\sigma_x = q_p$, is naturally restricted “from the top” by the limit pressure state, with geostatic or active boundary pressure restricting it “from the bottom”.

2. Influence of mechanical pre-consolidation on the railbed capacity

The influence that a rail has on the railbed is described by the Winkler model with uniform vertical rigidity U . Site tests point to random diversity of railbed rigidity underneath the cross-ties [10,15] and [19]. While taking into account the results of Polish and Russian research, the report [3] indicated the method of adjusting the calculations of cross-tie loads depending on diverse rigidity of the railbed, while employing the existing uniform model as shown in Fig. 2.

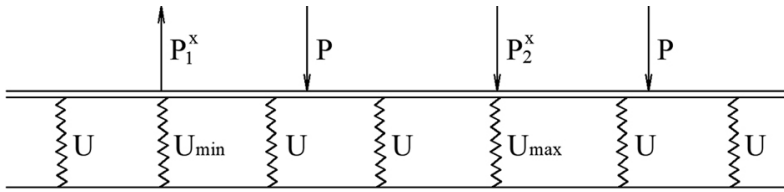


Fig. 2. Static diagram for calculating the load on the cross-ties depending on railbed rigidity

For any number of real loads P , the disturbed state is corrected by a set of fictitious forces P_i^x . The unfavorable distribution of the loads of the railbed will emerge underneath the cross-ties, which have the maximum rigidity of U_{max} , in the situation when the minimum rigidity of the neighboring cross-ties is U_{min} . The dynamic surplus of the load on the railway car axles is created by the vibration of the axle set (wheel set) as a result of non-uniform rigidity of the railbed and the vibration of the rail-car body itself, caused by longitudinal surface irregularities [1, 5, 7]. The dynamic surplus and the loads exerted by the weight of the railcars and of the load they carry are, as a result of the distribution presented in Fig. 2, transmitted to the railbed. For these reasons the value of the universally applied dynamic coefficient $K_v = P_d/P_s$ (P_d – the dynamic load on a rail, P_s – the static load on a rail) varies at the level of the railbed depending on whether a uniform or a varied rigidity model is used.

The relative, unfavorable loads exerted on the railbed in the case of the varied (alternately U_{max} and U_{min}) rigidity of the railbed occurring on the neighboring cross-ties was calculated in [6] as compared to the loads in the case of uniform rigidity of the railbed. The two- and four-axle cargo cars, characterized by the coefficient of variance $U = \pm 0.30$, which corresponds to poor condition of the rails, have been adopted for the analysis [9]. Irrespective of the number of axles, the relative coefficients were growth: $R_o/R_{o\ max} \approx 1.3$, gradient: $R_o - R_{min}/R_{o\ max} \approx 0.8$, where R_o is the maximum load on a railbed for varied rigidity, $R_{o\ max}$ – is the maximum load on a railbed for uniform rigidity, R_{min} – is the minimum load on a railbed for varied rigidity. For a constant railbed rigidity, the gradient is $\sim 50\%$ smaller. Varied load exerted on the railbed by adjacent cross-ties leads, potentially, to local displacement of the railbed (transverse beds as shown in Fig. 3).

Variation of the loads exerted on the railbed leads, in boundary states, to activation of displacement mechanisms, as defined by Prandtl, both in the protective layer and in the railbed itself (Fig. 4). The calculation scheme presented in Fig. 5 accounts for the displacement of the railbed (Fig. 3) and for the effects of pre-consolidation due to repetitive loads.

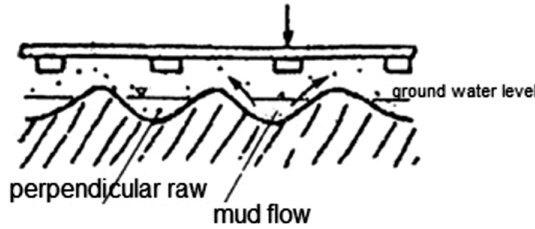


Fig. 3. Damage to the railbed due to insufficient load-bearing capacity as per [17]

As a result of pre-consolidation of the railbed during operation, the boundary resistance E_b (Fig. 5) is neutralized by the passive earth pressure $\sum_1^n \Delta\sigma_{xi} = q_p$, as per (1.4). For such reasons, passive earth pressure E_b includes only the dead weights of the layers. Based on the conditions of the equilibrium, for the maximum load gradient of 0.8 and the safety factor SF = 2 we arrive at the following estimation of the permitted load:

$$(2.1) \quad q_{dop} = \frac{1,9c_u \cdot \cos \varphi_u}{1 - \sin \varphi_u} + 0,5p_\gamma$$

where c_u and φ_u are the railbed strength parameters for total stress [14], p_γ – base compression generated by the load of the surface and of the railbed.

To illustrate the order of the values of pre-consolidation stress q_p , as compared to the stress q_z exerted on the railbed, we have calculated the above parameters for the data presented in Fig. 4 and Fig. 5: static load of the rail: $P_s = 105$ kN, speed of the cargo cars: $V = 80$ km/h, $K_v \approx 2.0$ (poor condition of the rails [9]), concrete cross-ties INBK-7D, thickness of the ballast $h = 30$ cm, thickness of the protective layer $t = 30$ cm, railbed strength parameters: $c_u = 50$ kPa, $\varphi_u = 10^\circ$, rail: S60.

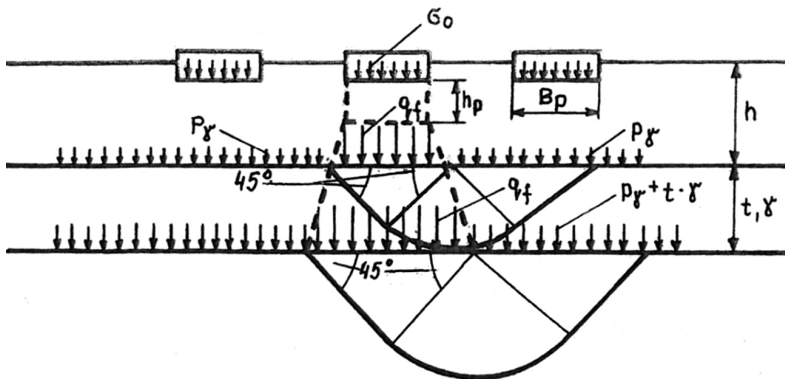


Fig. 4. Potential railbed displacement patterns due to maximum loads on the cross-ties (σ_0 – pressure of the railbed on the subgrade; p_γ – pressure of the unit weight of the pavement on the base layer; γ – bulk density of the base layer; t – thickness of the base layer; q_f – limit pressure on the railbed; B_p – railbed width; h_p – depth of the railbed dynamic pressure dissipation)

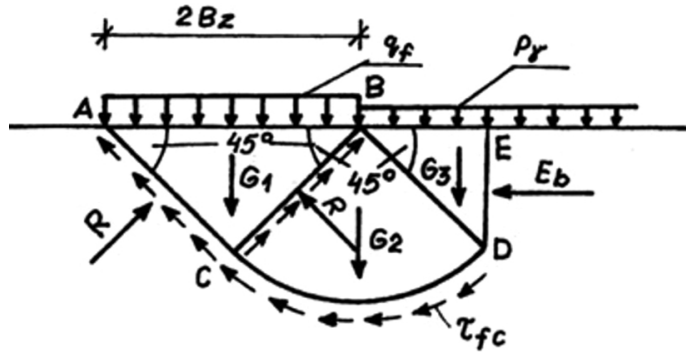


Fig. 5. Calculation of the boundary load capacity (q_f of the railbed; τ_{fc} – cyclic loading resistance of the soil; G_1, G_2, G_3 – unit weight of the displacement wedge solid; R – stiff zone reaction; E_b – passive pressure

For a classic Winkler model we obtained: dynamic stress exerted on the ballast in the sub-rail zone of the railbed of $\sigma_0 = 272$ kPa, dynamic stress on the railbed $q_z = 87$ kPa. While accounting for the heterogeneity $q'_z = 87 \cdot 1.3 = 113$ kPa. The cumulative pre-consolidation stress according to (8) is $q_p = 113 \cdot 1.2 = 135$ kPa. The unit passive earth pressure at the level of the railbed due to stress p_γ is $e_b = 0.16 \cdot 142 + 2 \cdot 50 \cdot 1.20 \approx 140$ kPa. The result of the calculations shows that an approximate balance between q_p and e_b exists in the railbed. The studies conducted by the Swedish company “Dynapack” recommend that the value q_p be assumed as the constant in the compacted layer (vertical displacement extent in this case).

The permitted load on the railbed according to (2.1) will be $q_{dop} = 115$ kPa, which is close to the maximum load of $q'_z = 113$ kPa. A Hungarian formula [11], derived on the basis of critical stress assumptions [12], is most often used to assess the permitted stress]:

$$(2.2) \quad q_{dop} = q_{kr} = \pi \cos \varphi_u c_u + p_\gamma \pi \sin \varphi_u$$

where the symbols used are the same as earlier. According to (2.2) $q_{dop} = 160$ kPa > 115 kPa. The relations between the formulas (2.1) and (2.2) for $p_\gamma = 0$ for various angles φ_u is shown in Table 1.

When introducing the critical stress formula, the elastic-plastic model is used where plasticization is restricted to the finite areas around the corners of the foundation (no displacement). It should be added that diverse rigidity of the railbed need not be symmetrical in respect of the longitudinal axis of the rails. Diverse rigidity could lead to transverse tilt of the cross-ties.

Table 1. Relation of the permitted stress to the angle of soil friction in the base

φ_u [°]	5	10	15	20	25	30
$\frac{q_{dop}}{q_{kr}}$	0.66	0.73	0.81	0.92	1.04	1.20

3. Pre-consolidation of railway embankments

Pre-consolidation of railway embankments occurs due compacting of soil layers while using static (vibration) rollers or vibration plates. Soil compacting equipment is characterized by specific technical parameters. With the use of these parameters, it is possible to determine the mean pressure that a device exerts on the layer q_z the cumulative pre-consolidation stress $q_p = 1.2 \cdot q_z$. For example, for a vibration roller HMM H180, with a mass of 12.2 t and vibration frequency of 30/40 Hz, the ground pressure is $q_z = 86$ kPa, the pre-consolidation pressure in the compacted layer: $q_p = 1.2 \cdot 86 = 103$ kPa. Fig. 6 presents the distribution of the pre-consolidation pressure values in a compacted embankment, demonstrating that the pre-consolidation pressure has significant influence on the stability of the embankment itself (whether reinforced or not reinforced), and that it increases shearing in the transmission layer and in the reinforced base.

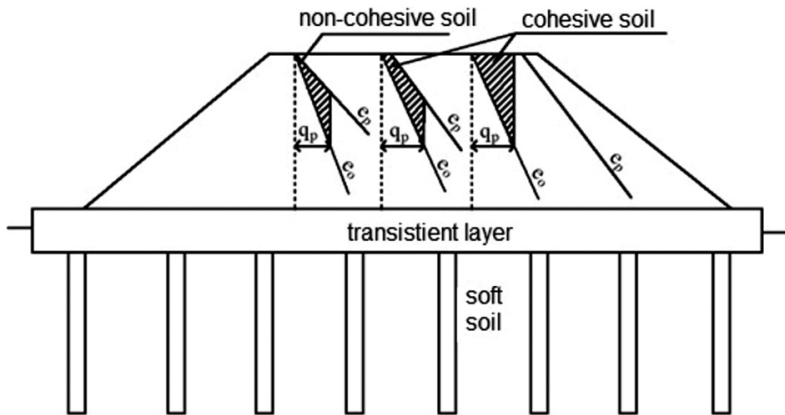


Fig. 6. Distribution of pre-consolidation pressures in an embankment; e_p – boundary passive earth pressure, e_0 – geostatic pressure, q_z – the cumulative pre-consolidation stress

The publication [2] recommends that the pre-consolidation pressure exerted on the retaining walls, having the value $q_p = 5-15$ kPa, be taken into account based on the distribution valid for non-cohesive soils (Fig. 6). The values are very conservative when compared to the actual values of pressure generated by heavy vibration rollers when compacting e.g. stabilized soils. Field research indicates that the pre-consolidation pressures (stresses) that are perpendicular to the direction of movement of the roller are approx. 3 times bigger compared to the longitudinal pressures [20]. Field tests [4] of an embankment made of all-in aggregate compacted with a roller VV-100 also resulted in the value of approx. 3.3 being achieved. The approximate uniformity of the pre-consolidation pressure is obtained by applying alternate method of compacting. The uniformity of compacting can be improved by using pulled rollers. Self-propelled rollers reduce the level of the boundary stress due to the horizontal force of adhesion at the point of contact between the roller and the ground.

4. Effects of historical mechanical pre-consolidation

In the case of subsoils, it is difficult to assess, in quantitative terms, the level of residual mechanical consolidation. In glacial periods (transgression, withdrawal) the substrate was subjected to displacement, which included shear and resistance zones. The range of the maximum value of the lateral expansion coefficient can be estimated using the following formula:

$$(4.1) \quad K_{\max} = \operatorname{tg}^2\left(45 + \frac{\varphi_e}{2}\right) + 2 \operatorname{tg} \alpha_c \operatorname{tg}\left(45 + \frac{\varphi_e}{2}\right)$$

where φ_e – the internal friction angle according to [12], α_c – reinforcement angle due to consolidation. The K_{\max} values, calculated for the soils demonstrating plasticity index of $I_p = 10, 20$ and 30% , are found in Table 2.

Table 2. K lateral expansion coefficient for various states of the subsoil

I_p [%]	10	20	30
ϕ_c [°]	26	22	18
K_{\max}	3.5	2.7	2.4

In the field the expansion coefficient K_{\max} is subject to restriction by the unit resistance e_p , which was the subject of the analysis in points 2 and 3. In the resistance zone the stress levels correspond to the extension, thus the values stated in Table 2 can be reduced by ca. 10%. The pattern of displacement, as shown in Fig. 7, was analyzed in order to estimate the depth of the influence that ice sheet had on the substrate. The boundary stress is:

$$(4.2) \quad q_f = \frac{1,40(1+m)[(1+m) + 1,41]c_u}{(1+m) + 0,17m^2}$$

the relative caving of the slip surface, with the symbols used being the same as in Fig. 7, is:

$$(4.3) \quad l/h_p = \frac{2+m}{0,18(1+m)}$$

The probable, mean slope β of the ice sheet slope angle was within the range of 30° ($m = 1.73$) to 15° ($m = 3.73$) due to the outflow of water from the glacier. The formula (4.1) rendered $l/h_p \approx 6.6$ in both cases. The following assumptions have been made to assess the height of the ice sheet H : bulk density of $\gamma \approx 15.0 \text{ kN/m}^3$, strength of the frozen subsoil in the case of uni-axial compression of $q_u \approx 800 \text{ kPa}$. Height of the ice sheet for $\beta = 30^\circ$, $H \approx 130 \text{ m}$ and $H \approx 180 \text{ m}$ for $\beta = 15^\circ$; with respective displacement depth values $h_p \approx 73 \text{ m}$ and 150 m . The depths at which glaciotectonic disturbance occurs are much bigger as compared to the level at which the facilities/structures are set. The mechanics of the continental plates [20] shows that the value of the optimal l/h_p ratio for the biggest uplift rate is:

$$(4.4) \quad l/h_p \approx 3,14\sqrt{K}$$

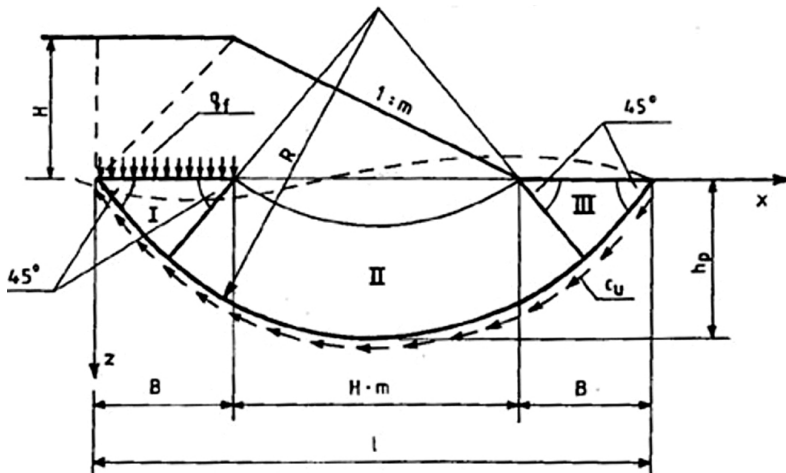


Fig. 7. Diagram of subsoil displacement by the glacier: H – ice sheet height; l – displacement width; B – width of the pressing zone; h_p – depth of the displacement zone; R – radius of the slip surface

Using formula (4.4), for $K = 2.5$ and 3.5 (Table 2), the results of ca. 5.0 and 6.0 respectively were obtained. Thus, the conclusion that the uplift phase changes to displacement phase for the same ratio l/h_p . What is left is the matter of estimating the minimum value of the lateral pressure ratio which originated the uplift phase. For the needs of the analysis a diagram for the heavy and incompressible layers has been adopted as per Fig. 8.

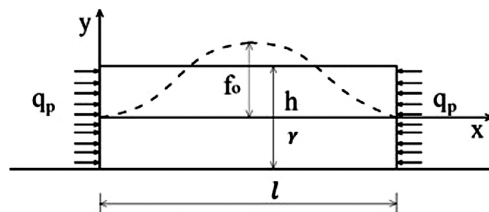


Fig. 8. Diagram showing uplift of the near surface layer: h – thickness of the near surface uplift layer; f_0 – uplift amplitude; γ – bulk density of the layer; l – width of the displacement zone

The load is created by the deadweight as well as the residual pre-consolidation pressure q_p . The uplift form can be co-sinusoidal ($y = 0,5f_0(1 - \cos \frac{2\pi x}{l})$) or sinusoidal ($y = f_0 \sin \frac{\pi x}{l}$). During field tests [16] the recompression of the trench for the underground line, in tertiary clay, was close to a sinusoidal form. Assuming equality of the influence of the pressures q_p and the gravitational forces as the starting point, regardless of the form of the uplift, we arrive at $K_{\min} = 2.0$. Thus, a recompression wave is created as a result of relaxation of the pre-consolidation stresses underneath the head of the glacier or in its foreground as well as at the bottom of a deep trenches. The shifts generated by the recompression add up to the sum of oedometric deformations and uplifts. The consequences of presence of residual pre-consolidation stress are visible in the form of soil creep and landslides which

occur in boulder clay on river valley slopes. Lateral erosion of rivers leads to washing away of the escarpments which serve as buttresses, resulting in uncovering of soil areas which were subjected to a higher pre-consolidation pressure. Such phenomena can, for example, be observed in the Bug and Narew River valley by the Debe dam or on Plock's slope. Fig. 9 illustrates the potential consequences of decompression of the bottom of deep trenches. As a result of relaxation of the pre-consolidation stress q_p , the K expansion coefficient reaches the minimum value of $K \approx 2.0$.

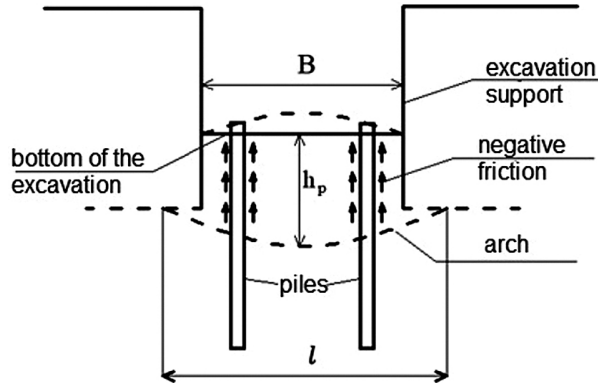


Fig. 9. Diagram presenting the decompression of the bottom of a deep trench: B – excavation width; l – width of the arch zone

According to the formula (4.4), l/h_p approaches the value ≈ 4.4 . Thickness of the decompressed zone of the elevated areas will in such a case be:

$$(4.5) \quad h_p = \frac{l}{4.4}$$

where l denotes the width of the arch. For example, for a trench width of $B = 15$ and 20 m and while assuming that $l \approx B$, the obtained results are respectively $h_p = 3.2$ and 4.5 m.

The mean immersion of the retaining walls below the trench bottom level is 4–5 meters, which means that the depressed zone can stretch beyond the ends of the retaining walls. If the slab is founded on piles, the piles can be exposed to stretching in their upper ends during the initial phase of the construction works (due to negative friction on the side surface as shown in Fig. 9). Paper [19] quotes the results of the field tests performed by Sommer and Katzenbach at the construction site in Frankfurt (Germany) where negative friction was recorded in the upper part of the side surface of the pile for loads of up to $\sim 50\%$ of the total load. Presence of the negative friction on the side surface is increased by the settlement of the slab and pile foundations. Formula (4.5) also enables assessment of the extent of the uplift in the subsoil (base) of a high heap slope. For the depths of $h_p = 73$ and 150 m, the range of the uplift will be respectively 320 and 660 m.

5. Comments regarding selected geotechnical issues

In laboratories soil is often condensed to a pre-defined γ_d in bigger containers. Condensing of soil by means of e.g., compacting results in the pre-consolidation pressure being introduced. Publication [12] quotes the values of critical depths (reliable interpretation of results) for dynamic probes DP, FVT. The tests were performed in cylindrical containers with consolidated sand. A question remains to be answered: do the critical depths also depend on the degree of compacting, which in practice means that they depend on the pre-consolidation pressures applied when compacting the soils? The notion of critical depth should be linked to the linear relationship between the friction on the sidewall and resistance under the pile foot, respectively at the depths of up to 5 and 10 meters from the surface of the load-bearing soil.

References

- [1] T. Basiewicz, *Nawierzchnia kolejowa z podkładami betonowymi*. Warszawa: WKiŁ, 1969.
- [2] R. Bobe and H. Hubáček, *Boden mechanic*. Berlin: VBB Verlag für Bouveesen, 1984, pp. 186–199.
- [3] M. Bukowski and A. Kurcz, “Centralny Program Badań Podstawowych, Wpływ obciążeń torowiska kolejowego na zachowanie się gruntowego ośrodka podtorza, Sprawozdanie roczne 1988”. Instytut Dróg i Mostów Wydz. Inżynierii Lądowej PW (not published).
- [4] M. Bukowski and A. Kurcz, “Centralny Program Badań Podstawowych, Wpływ obciążeń torowiska kolejowego na zachowanie się gruntowego ośrodka podtorza, Sprawozdanie roczne 1989”. Instytut Dróg i Mostów Wydz. Inżynierii Lądowej PW (not published).
- [5] M. Bukowski, “Interpretacja modelu Winklera i dynamiczne parametry toru kolejowego”, *Archives of Civil Engineering*, no. 4, pp. 351–370, 1990.
- [6] M. Bukowski, “Wpływ podkładek wibroizolacyjnych w podkładach betonowych na wzajemne oddziaływanie pojazdu, nawierzchni i podtorza”, *Problemy Kolejnictwa*, no. 150, p. 59–88, 2010.
- [7] E. Dembicki and B. Rymśza, “Obliczanie parcia i oporu gruntu według Eurokodu 7 (postęp czy regres)”, *Inżynieria Morska i Geotechnika*, no. 3, pp. 237–246, 2015.
- [8] J. Eisenmann, Ed. *Forschungsarbeiten auf Gebiet des Eisenbahn – und Stressenoberbaus*. Berlin-München-Düsseldorf: Verlag von Wilhelm Ernst und Sohn, 1974, pp. 38–62.
- [9] M. A. Frizman, *Tor kolejowy i jego współpraca z pojazdami*. Warszawa: Wydawnictwo Komunikacji i Łączności, 1983, pp. 27–90.
- [10] L. Karafiath, *Einfluss der Verfestigung und der Zeitdauer der Lataufbringung auf die Grenzbelastung des Baugrundes* Gevenkbuch für prof. dr. J. Jaky. Akamedie Kiado Budapest, 1955, pp. 101–119.
- [11] M. Lipiński, “Wybrane kryteria określania parametrów gruntów naturalnych”, *Inżynieria Morska i Geotechnika*, no. 4, pp. 267–285, 2012.
- [12] PN-83/B-03010 Ściany oporowe. PKN, 1984.
- [13] ORE, D-71, Stresses in the rails, the balast and in the formation resulting from traffic loads, Rep.8, 11, 12.
- [14] R. Porębski, “Dynamiczne oddziaływania nawierzchni na podtorze podczas ruchu pociągów”, PhD. thesis, Politechnika Poznańska, Instytut Inżynierii Lądowej, Poznań, 1983.
- [15] B. Skrzyński, *Podtorze kolejowe*. Warszawa: Kolejowa Oficyna Wydawnicza, 2010, pp. 208–209.
- [16] A. Szymański and W. Wolski, *Badanie stanu naprężeń i cech fizykomechanicznych gruntów w otoczeniu obiektów metra*. Warszawa: SGGW, Katedra Geotechniki, 1992.
- [17] A. Tejchman, K. Gwizdała, I. Dyka, J. Świniński and A. Krasieński, *Nośność i osiadanie fundamentów palowych*. Politechnika Gdańska, 2001.
- [18] T. Uemura, S. Minutani, *Geologiczne struktury*. Moskwa, 1990, pp. 188–238.
- [19] A. Wasiutyński, *Badania nad odkształceniami sprężystymi nawierzchni kolejowej i naprężeniami w szynach na posterunku doświadczalnym Włochy P.K.P.* Warszawa: Ministerstwo Komunikacji, 1937.
- [20] R. Whitman and T. Lambe, *Soil mechanics*, vol. 1. Warszawa: Arkady, 1977, pp. 243–285.

Wpływ prekonsolidacji mechanicznej gruntów na ocenę stanu naprężeń w praktyce geotechnicznej

Słowa kluczowe: konsolidacja dynamiczna, konsolidacja lodowcem, mechaniczne zagęszczanie, prekonsolidacja

Streszczenie:

Projektowanie geotechniczne obejmuje prace budowlane, podczas których grunt poddawany jest powtarzalnym naprężeniom pionowym w procesie zagęszczania, np. w przypadku nasypów czy składowisk odpadów. W sytuacji, gdy naprężenie przekroczy próg prekonsolidacji, następuje kumulacja trwałych odkształceń, zwykle poziomych, co powoduje dodatkowe naprężenia boczne. W artykule zaprezentowano, potwierdzoną wieloletnią praktyką, zasadę wyznaczania naprężeń poziomych powstałych w wyniku wstępnego zagęszczenia mechanicznego. Niezależna analiza matematyczna potwierdziła, że zakresy graniczne cyklicznego współczynnika naprężenia bocznego odpowiadają aktywnym lub reaktywnym stanom odkształcenia. W praktyce geotechnicznej istotne są stany reaktywne, w których następuje dodatkowa kumulacja odkształceń bocznych w gruncie.

Received: 2023-11-09, Revised: 2024-03-05